

---

# Vibration-based Damage Detection with Uncertainty Quantification by Structural Identification using Nonlinear Constraint Satisfaction with Interval Arithmetic

Journal Title  
XX(X):1-18  
©The Author(s) 2018  
Reprints and permission:  
sagepub.co.uk/journalsPermissions.nav  
DOI: 10.1177/ToBeAssigned  
www.sagepub.com/  


Timothy Kernicky<sup>1</sup>, Matthew Whelan<sup>1</sup>, and Ehab Al-Shaer<sup>2</sup>

## Abstract

Structural identification has received increased attention over recent years for performance-based structural assessment and health monitoring. Recently, an approach for formulating the finite element model updating problem as a Constraint Satisfaction Problem has been developed. In contrast to widely used probabilistic model updating through Bayesian inference methods, the technique naturally accounts for measurement and modeling errors through the use of interval arithmetic to determine the set of all feasible solutions to the partially described and incompletely measured inverse eigenvalue problem. This paper presents extensions of the constraint satisfaction approach permitting the application to larger multiple degree-of-freedom system models. To accommodate for the drastic increase in the dimensionality of the inverse problem, the extended methodology replaces computation of the complete set of solutions with an approach that contracts the initial search space to the interval hull, which encompasses the complete set of feasible solutions with a single interval vector solution. The capabilities are demonstrated using vibration data acquired through hybrid simulation of a forty-five degree-of-freedom planar truss, where a two-bar specimen with bolted connections representing a single member of the truss serves as the experimental substructure. Structural identification is performed using data acquired with the undamaged experimental member as well as over a number of damage scenarios with progressively increased severity developed by exceeding a limit state capacity of the member. Interval hull solutions obtained through application of the nonlinear constraint satisfaction methodology demonstrate the capability to correctly identify and quantify the extent of the damage in the truss while incorporating measurement uncertainties in the parameter identification.

## Keywords

Structural Identification, Finite Element Model Updating, Damage Detection, Partially Described Inverse Eigenvalue Problem, Interval Arithmetic, Vibration-Based Structural Health Monitoring

## Introduction

In recent years, numerous methods have emerged for the updating of structural matrices using vibration data obtained from experimental and operational modal analyses. These updated stiffness and mass matrices have in turn been proposed for inferring properties of in-service structures and predicting behavior and performance to aid in decision making. Despite successful demonstrations of finite element model updating on full-scale structures, there are several persistent challenges. The primary challenge is that model updating is an inverse problem that is greatly affected by numerous sources of uncertainty including: the selection of uncertain parameters, modeling assumptions, and measurement uncertainties<sup>1</sup>. In addition to being an inverse problem, the finite element updating problem is typically partially described, wherein only a subset of the natural frequencies of the model are measurable given the bandwidth limitations of transducers<sup>2</sup>. Similarly, from a practical standpoint, it is impossible to measure every degree of freedom represented in the analytical model, so the experimentally derived mode shapes are also inherently incomplete. Understanding how the

effect of the limited measurements and measurement uncertainties propagate into the identified parameter space to quantify the confidence in the results is paramount for decision making purposes, especially when the application relates to vibration-based damage detection.

In the past decade, the predominant approach for model updating in the presence of uncertainties is a class of methods referred to as probabilistic model updating<sup>3</sup>. Probabilistic model updating employs statistical methods to provide a family of potential structural models<sup>4</sup>, instead of determining a single best deterministic solution, that incorporate measurement

---

<sup>1</sup>University of North Carolina at Charlotte, Department of Civil and Environmental Engineering,  
9201 University City Boulevard, Charlotte, NC 28223-0001 U.S.A.

<sup>2</sup>University of North Carolina at Charlotte, Department of Software and Information Systems,  
9201 University City Boulevard, Charlotte, NC 28223-0001 U.S.A.

### Corresponding author:

Matthew Whelan, University of North Carolina at Charlotte,  
Department of Civil and Environmental Engineering,  
9201 University City Boulevard, Charlotte, NC 28223-0001 U.S.A.  
Email: M.Whelan@uncc.edu

uncertainties in the posterior distributions of the model parameters. However, these methods require assumed probability density functions, a likelihood function with associated weighting coefficients to express relative importance of the natural frequency and mode shapes residuals, and rely heavily on the stochastic simulation method chosen<sup>5,6</sup>. In addition, probabilistic methods can be computationally expensive, often requiring tens of thousands of simulations<sup>5</sup>, even when the number of uncertain parameters is relatively small<sup>7</sup>. In general, probabilistic model updating presents several challenges including: the results remaining highly dependent on the initial finite element model and the selection of uncertain parameters included in the updating<sup>7</sup>, direct matching of modes is often required<sup>8</sup>, and the weights assigned to residuals in the objective function greatly affect the solution space<sup>7,9</sup>.

There have been numerous applications of probabilistic model updating for vibration-based damage detection<sup>7,10–17</sup>, which have underlined the importance of addressing remaining challenges for practical application. An early study on probabilistic model updating determined that some identified parameter sets, while providing strong correlations with the experimental modal parameter estimates, may erroneously locate and quantify damage in the presence of measurement and modeling errors<sup>10</sup>. The identifiability of damage is dictated by several factors including: the number and location of measurement sensors deployed during the vibration test and the quality of the measurement data. The first factor determines whether the problem is identifiable or unidentifiable, which is dependent on there being more unique modal measurements than the number of uncertain parameters in the model<sup>14</sup>. However, it has also been shown that employing more modes in the identification does not guarantee better damage identification results<sup>18</sup>. Mustafa and Matsumoto<sup>16</sup> explored practical application of Bayesian model updating for detection of simulated damage of a single diagonal member of a truss bridge and indicated that identification of local damage was not possible using only global modes. In addition, the authors indicated that detection of local damage may only be possible if the modal properties utilized in the finite element model updating scheme are significantly affected by the damage. Huang et al.<sup>15</sup> outlined several uncertainties associated with vibration-based Bayesian model updating and how those uncertainties affect the ability to successfully identify damage. The authors stated that quality of the measured data has the largest effect on the ability to identify damage and demonstrated that successful identification of low level damage may not be possible even if the measurement noise is low. Utilization of damage identification results in such cases may lead to incorrect conclusions regarding the early onset or absence of damage. Likewise, high levels of measurement noise preclude successful damage detection. Consequently, it was stated that an appropriate threshold must be chosen to distinguish damaged elements from undamaged elements, which itself is a practical challenge. Setting the threshold low, which

increases the detection of damaged elements, may falsely identify undamaged elements as damaged. Conversely, if the damage threshold is set too high, there is a high probability of missing actual damage. In addition, since the sensitivity of the modal parameters estimates to the individual uncertain parameters in the model to be updated may vary significantly, the threshold for damage detection may also need to vary for individual structural members.

Recently, alternatives to probabilistic model updating have been introduced that also offer the capability to account for measurement uncertainties are based on interval methods<sup>19</sup>. Interval analysis techniques have an advantage over probabilistic methods in that they do not require assumptions regarding the probability density functions of uncertain parameters and are capable of completely exploring the feasible parameter space without using discrete sampling techniques or a modal measure of fit function. Gabriele et al.<sup>20</sup> presented one of the first studies employing interval analysis to place bounds on uncertain parameters, measurements, and modeling errors. The authors of that study utilized the inclusion property of interval analysis to place bounds on uncertain model parameters for damage identification. Wang et al.<sup>21</sup> employed interval analysis for damage detection using a membership-set identification method. The two-step sensitivity-based interval model updating technique employed in that study used static displacement measurements across different load cases to identify uncertain stiffness parameters. The intersection of the updated interval stiffness parameter vectors for each load case resulted in tight bounds on the stiffness parameter estimates. In a subsequent study<sup>22</sup>, measured natural frequencies as well as uncertain acceleration responses were employed for damage detection using the same two-step interval finite element model updating approach with membership-set identification. It was concluded that utilizing more than a single type of measured data (i.e. just static displacements) resulted in higher accuracy of damage identification. Khodaparast et al.<sup>23</sup> explored the use of a meta-model using the Kriging predictor for model updating, which was implemented successfully for interval model updating of a three degree-of-freedom mass-spring system. However, although the approach presented utilizes interval model updating, the approach addresses the field of stochastic model updating, where multiple sets of data from nominally identical structures are employed for identification of parameter variability, instead of identifying uncertain parameters for a single structure. Fang et al.<sup>24</sup> also presented a stochastic model updating method, which adopted the use of measured eigenvalues as well as eigenvectors. The authors of that study indicated that the proposed interval response surface method (IRSM) provided higher precision than the Kriging predictor and that it was more computationally efficient given that interval arithmetic operations are easily performed on the response surface model. Gabriele and Valente<sup>25</sup> prescribed modal properties as intervals and model updating was performed using branch and bound

processes until the prescribed modal intervals were encompassed by the modal properties of the interval FE model. In an extension of that work, the authors introduced mode shapes within the model correlation through the use of the Modal Assurance Criterion (MAC)<sup>26</sup>. The exploration of the parameter space was again based on branch and bound techniques, although the authors concluded that the convergence was slow compared to sensitivity-based optimization techniques and the application was limited to a small numerical beam model.

A recent effort has been made to combine both probabilistic and interval methods for damage detection using a modified Metropolis-Hastings algorithm with interval measurements<sup>17</sup>. In that study, intervals are created around the parameters sampled by the MH algorithm and then two separate finite element analyses are performed using the lower and upper bounds for the parameters to obtain the lower and upper bounds for the dynamic response of the model. In the process, the Markov chain only moves to a new position if the intersection of the response bounds calculated from the finite element models with the interval measurements is non-empty. Although the method was shown to reduce the computational burden of both the probabilistic and interval-based methods, it still required over 10,000 finite element analysis runs.

The updating procedure in the majority of the existing probabilistic and interval-based model updating techniques relies on global optimization of an objective function that is an amalgamation of natural frequency and mode shape residuals across a number of measured modes and does not guarantee that the modal properties of the updated model are contained within the uncertainty bounds of the experimental measurements. To address this shortcoming, model updating has recently been cast as a constraint satisfaction problem with interval arithmetic and contractor programming to provide the ability to efficiently characterize the set of all feasible solutions to a structured inverse eigenvalue problem and the capability to solve under-determined and non-unique problems in the presence of measurement uncertainties<sup>27</sup>. In addition to full exploration of the parameter space, the method does not require weighting of correlation residuals, which can have drastic effects on the identification. To date, the method has been numerically verified and experimentally validated using a six degree-of-freedom laboratory shear building model.

This paper introduces adaptations to the aforementioned approach to finite element model updating with interval arithmetic and contractor programming that are necessary to permit the application of the methodology to larger multiple degree-of-freedom (MDOF) system models with larger sets of uncertain parameters. The extension of the methodology produces interval estimates for the uncertain parameters in the form of an interval hull that is guaranteed to enclose the set of all feasible solutions to the structured inverse eigenvalue problem with partially described and incompletely measured eigeninformation pairs corrupted by

measurement noise and uncertainty. The methodology is demonstrated for structural identification of a truss using experimental data obtained through hybrid testing. The experiments are then extended to several cases of progressive damage severity at a bolted connection to demonstrate the capability of the method to correctly identify the onset, location, and severity of damage in the presence of measurement uncertainties.

## Finite Element Model Updating Using Nonlinear Constraint Satisfaction

In this section, the methodology developed by the authors for structural identification using nonlinear constraint satisfaction in Kernicky et al.<sup>27</sup> is briefly reviewed and then extensions of the methodology are introduced to facilitate the application to larger multiple degree of freedom system models.

The finite element model updating problem is most commonly applied to multiple degree of freedom system models using the undamped natural frequencies and mode shapes. The generalized eigenvalue problem for undamped linear systems is

$$K\Phi - M\Phi\Omega = 0 \quad (1)$$

where  $M$  and  $K$  are the mass and stiffness matrices,  $\Omega$  is the diagonal matrix of eigenvalues ( $\omega_n^2$ , where  $\omega_n$  are the undamped natural frequencies), and  $\Phi$  are the corresponding eigenvectors, or mode shapes, represented as columns of the matrix. The ultimate goal of the finite element model updating problem is to solve for a set of parameters within  $M$  and  $K$ , which are  $n \times n$  square matrices, given a set of estimated eigenvalues and eigenvectors obtained through physical testing of the structure. However, most cases of model updating are partially described where only  $m < n$  eigenpairs are measured due to bandwidth limitations of the sensing equipment and practical limitations within the system identification of the modal parameters from the vibration test data. In addition, only  $s < n$  degrees of freedom of the corresponding numerical model are typically measured in the physical testing, leading to incompletely measured mode shapes. In the context of this partially described eigenvalue problem with incompletely measured modes, the matrix equation can be partitioned as:

$$K_{n \times n} \begin{bmatrix} \Phi_{s \times m}^M \\ \Phi_{(n-s) \times m}^U \end{bmatrix} - M_{n \times n} \begin{bmatrix} \Phi_{s \times m}^M \\ \Phi_{(n-s) \times m}^U \end{bmatrix} \Omega_{m \times m} = 0_{n \times m} \quad (2)$$

where  $\Phi_{s \times m}^M$  are the rows of the measured components of the  $m$  measured mode shapes and  $\Phi_{(n-s) \times m}^U$  are the rows of the unmeasured components of the same  $m$  measured mode shapes. In this study, the structural matrices are explicitly formed through elemental

contributions as:

$$\left[ K_o + \sum_{j=1}^{N_K} \alpha_j K_j \right] \begin{bmatrix} \Phi_{s \times m}^M \\ \Phi_{(n-s) \times m}^U \end{bmatrix} - M_{n \times n} \begin{bmatrix} \Phi_{s \times m}^M \\ \Phi_{(n-s) \times m}^U \end{bmatrix} \Omega_{m \times m} = 0_{n \times m} \quad (3)$$

where  $\alpha_j$  is a scalar multiplier applied to a basis matrix,  $K_j$ , that provides the stiffness contributions of the  $j$ -th member of the model, while  $K_o$  represents the contributions of any members in the model not subject to updating. In such a formulation, the unknowns in the inverse eigenvalue problem are the  $N_K$  scalar multipliers for the member stiffness contributions subject to updating and the  $(n-s) \times m$  unmeasured components of the eigenvectors. Employing interval arithmetic, the constructed stiffness matrix can be developed as an interval matrix,  $K^I$ , where the uncertain stiffness scalars in the model are encoded as intervals

$$\alpha = [\underline{\alpha}, \bar{\alpha}] \quad (4)$$

where  $\underline{\alpha}$  is the lower bound to the interval for the uncertain parameter and  $\bar{\alpha}$  is the upper bound. Likewise, the unknown eigenvector components are treated as intervals

$$\Phi_{(n-s) \times m}^U = [\underline{\Phi}_{(n-s) \times m}^U, \bar{\Phi}_{(n-s) \times m}^U] \quad (5)$$

In this formulation, intervals are also employed to account for measurement uncertainties by relaxing the measured modal parameters from crisp scalars to intervals centered around the experimental measurements. To do this, each partially described eigenvector,  $\phi_r^M$ , is first scaled to unity maximum amplitude and then an interval is developed around all components except the one with maximum amplitude as:

$$\phi_{i,r}^{I,M} = [\underline{\phi}_{i,r}^M, \bar{\phi}_{i,r}^M] = \begin{cases} [\phi_{i,r}^M - \chi_{i,r}, \phi_{i,r}^M + \chi_{i,r}] & \text{if } \phi_{i,r}^M \neq 1 \\ [1, 1] & \text{if } \phi_{i,r}^M = 1 \end{cases} \quad (6)$$

where  $\chi_{i,r}$  is a specified radius for the intervals. The reason why the component with the maximum amplitude is not relaxed is to establish that component as a reference since the amplitude of an eigenvector is not unique. In a similar manner, the experimentally measured eigenvalues can be prescribed as intervals:

$$\omega_r^I = [\underline{\omega}_r, \bar{\omega}_r] \quad (7)$$

to reflect uncertainty in the experimental estimates of the natural frequencies. Relaxation of the experimental estimates to account for measurement and modeling uncertainties allows for Equation 3 to create a set of  $n \times m$  constraint equations.

The extent of the relaxation dictates the satisfiability of the constraint equations. If the radius of the intervals is too narrowly prescribed in the presence of measurement and modeling uncertainties, then satisfiability of the constraints will not be met and no

solution will be present. Conversely, if the radius is too wide, then the solution space may simply encompass the initial ranges of the uncertain variables. Choosing the extent of relaxation may either be performed iteratively based on the solvability of the constraints or may be determined by a measure of uncertainty in the modal parameter estimates. For the latter case, when multiple sets of modal parameter estimates are available, the radius of relaxation,  $\chi$ , may be represented by the standard deviation from the mean of each modal parameter estimate,  $\sigma$ .

In the original formulation of this methodology<sup>27</sup>, an additional constraint termed the eigenvalue inclusion constraint was introduced to ensure that the prescribed eigenvalues are contained within the interval eigenvalues of the identified interval stiffness and mass matrices, which cannot be ensured solely by the constraint equations in Equation 3. For small system models, the inclusion test can be implemented by substituting each of the measured eigenvalues into the characteristic equation formed from the determinant:

$$|K^I - (\omega_r^I)^2 M| = \left| K_o + \sum_{j=1}^{N_K} [\alpha_j, \bar{\alpha}_j] K_j - (\omega_r^I)^2 M \right| = 0 \quad (8)$$

### Constraint Satisfaction with Interval Arithmetic

A fundamental difference between the developed methodology and most existing approaches for model updating is that, instead of casting the problem as an optimization problem using an objective function or modal measure of fit function, the approach solves for the complete feasible parameter space that satisfies the constraints formed through Equations 3 and 8. Formally, a constraint satisfaction problem aims to determine all possible solutions for a set of variables,  $V$ , in a prescribed domain,  $D$ , over a set of constraints,  $C$ , through systematic search and constraint propagation<sup>28</sup>. Systematic search may be viewed as a branch and bound approach explored as a tree structure, where the root node represents the entire problem. Subsequent nodes of the tree represent subproblems of the root node, which differ in variable assignment. If during evaluation of a node it is determined that there is constraint violation, backtracking is performed to find a new satisfiable assignment and the subtree below the failed node is pruned from the search space. In this way, systematic search improves on the brute force method of trying all possible variable combinations. However, simple backtracking is an ‘‘uninformed’’ approach and is not effective for problems with significant dimensionality. One of the main challenges associated with solving a CSP is improving the performance of the search methods such that local inconsistencies are eliminated. Local inconsistencies are potential partial solutions that satisfy the constraints, but cannot be extended by choosing values for some of the uninstantiated variables. In other words, selecting a value for a uninstantiated variable would cause failure of the node. One method

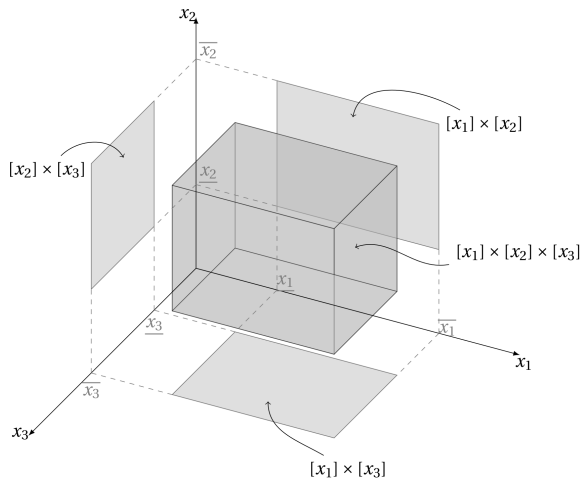


**Figure 1.** An interval vector, or box, generated from the product of three intervals

to enforce local consistency is arc consistency, which provides a swift method for constraint propagation<sup>29</sup> that discards values, or combinations of values, if their assignment violates some set of constraints. Eliminating erroneous assignments reduces the size of the search space to be explored by propagating the implications of a constraint on one variable onto the other variables. Combining the processes of systematic search and arc consistency is called Constraint Programming<sup>28,30,31</sup>.

Interval arithmetic may be incorporated into constraint programming so that variables and the relationships among them in the constraint equations are defined as intervals<sup>32</sup>, which provides a natural way to place bounds on numerical rounding errors and measurement uncertainties. Parameters defined as intervals instead of crisp scalars are able to assume any value within the interval. An interval  $[x]$  is a subset of the real numbers,  $\mathbb{R}$ , that can be represented using a pair of real numbers  $[\underline{x}, \bar{x}]$  to denote the interval  $\underline{x} \leq x \leq \bar{x}$ . If the endpoints,  $\underline{x}$  and  $\bar{x}$ , of an interval are equal, the interval is known as *degenerate* and may be represented as a single real number. The Cartesian product of intervals creates an  $n$ -dimensional box, or interval vector, that belongs to the set  $\mathbb{IR}^n$ . This product is defined as

$$[\mathbf{x}] = [x_1] \times [x_2] \times \cdots \times [x_n] \quad (9)$$

and is illustrated graphically in Figure 1 for the product of three intervals.

The objective of the interval constraint programming problem is now to identify all interval vector solutions that satisfy the set of constraint equations within the bounded domains for each set of interval variables. Note that in dealing with continuous domains, arc consistency cannot be held due to limitations on machine precision so hull consistency<sup>33</sup> is introduced. Hull consistency may be viewed as a coarse extension of arc consistency that requires arc consistency to only be satisfied at the lower and upper bounds of the interval variable domains. A constraint is hull consistent with respect to a box if, for each bound of the domain of an interval variable,

there is a real valued combination of variables satisfying the constraint.

### Contractor Programming

A programming method that integrates interval analysis and constraint programming, termed Contractor Programming<sup>34</sup>, has recently been developed to address interval constraint programming problems. Contractors are powerful mathematical operators that take an  $n$ -dimensional box as an input and contract the domain according to a set of constraints. The formal definition of a contractor and its properties are defined as follows<sup>35</sup>:

A contractor ( $C$ ) is a function from  $C: \mathbb{IR}^n \rightarrow \mathbb{IR}^n$ , where  $\mathbb{IR}$  is interval over reals, with the following properties:

- $\forall [\mathbf{x}] \in \mathbb{IR}^n \quad C([\mathbf{x}]) \subset [\mathbf{x}]$ ; where  $C([\mathbf{x}])$  represents box  $[\mathbf{x}]$  after contraction
- $C([\mathbf{x}]) \cap System = [\mathbf{x}] \cap System$

The first property guarantees that the algorithm is sound in that the contracted box is a subset of the original, while the second property states that no potential solution is lost after the contraction is performed. Following contraction, the interval vector can be bisected into a subset of smaller boxes and the contractors can be applied to further characterize the solution space.

For the current study, the authors have developed an interface between the MATLAB interactive environment<sup>36</sup> and the IBEX 2.1.17 C++ library<sup>37</sup> to construct and parameterize the structural stiffness and mass matrices, develop mechanics-based constraint equations, pass the formulated CSP to the IBEX solver, and parse the interval vector solutions generated by the contraction algorithm for subsequent analysis. In the following subsection, motivation for casting the updating problem as one of constraint satisfaction is developed through a simple illustrative example. Then, issues with the scalability of the original formulation are addressed through a novel extension of the methodology suitable for application to larger MDOF system models. Finally, application of the methodology to a 45 degree-of-freedom truss model with experimental hybrid testing data is presented to demonstrate its capabilities for vibration-based damage detection.

### Illustrative Example on a 3DOF Shear Building Model

As motivation for the methodology presented in this paper, consider the small three degree-of-freedom shear building model with accompanying structural matrices presented in Figure 2. For the baseline model, the stiffnesses were assigned as  $k_1 = k_2 = k_3 = 1$ . The sparsity structure of the elemental contributions to the stiffness matrix from each linear elastic spring are explicitly defined in the structured matrices and constraint equations for the dynamic properties of the structure can be developed using Equations 3 and 8.

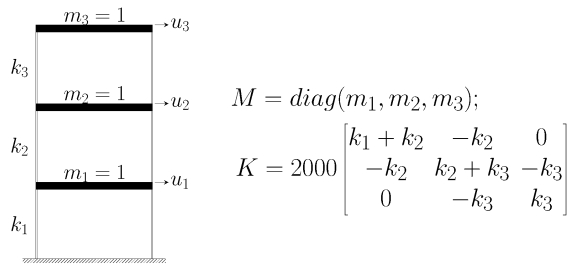


**Figure 2.** Three degree-of-freedom mass-spring model used to demonstrate structural identification using nonlinear constraint satisfaction with interval arithmetic and contractor programming

To add uncertainty to the measurements, 15 sets of synthetic modal parameter estimates with a standard deviation of 0.01 were generated around the natural frequencies and mode shapes derived from the baseline model. Constraint equations were developed with the means and standard deviations of the synthetic measurement data used to prescribe uncertainty in the constraint equations. Similar to the six degree-of-freedom illustration presented in Kernicky et al.<sup>27</sup>, a case with partially described eigenvalues and incompletely measured mode shapes was explored by limiting the eigeninformation to the first two modes of the structure and mode shape measurement to only degrees of freedom  $u_2$  and  $u_3$ . The search space for the three unknown stiffness parameters was bounded to  $k_i \in [0, 3]$ , while the search space for the unmeasured mode shape components was bounded to  $\phi_{i,j} \in [-10, 10]$ . For this example, an interval precision of 0.01 for the uncertain stiffness assignments and the unmeasured mode shape components was assigned as stopping criteria for the solver. The measurement uncertainty applied to the natural frequencies and measured mode shape components was prescribed as  $\pm \frac{1}{4}\sigma$ . Figure 3 displays the fully characterized subpaving of the space as mapped by the IBEX nonlinear constraint satisfaction solver, which identified 2492 feasible interval solutions in two distinct basins in about 5 seconds. It should be noted that all of the solutions found are correct solutions to the inverse eigenvalue problem subject to the partially described, incompletely measured, and noisy eigeninformation. This is illustrated in Figure 3, which presents the natural frequencies and mode shapes associated with a representative feasible solution taken from each basin. Both representative feasible solutions correctly reproduce the limited measurements, consisting of the first two natural frequencies and the corresponding mode shapes measured at only the second and third elevations of the structure. Naturally, there are significant differences in the unmeasured modal parameters and it would be difficult to determine which solution is more appropriate and, correspondingly, whether damage is present in the structure. For example, while it can be confidently stated that no significant damage is present in  $k_3$ , the same confidence cannot be placed on  $k_1$  and  $k_2$  given the uncertainty associated with each parameter. As a consequence of

the effect of the limited and uncertain measurement data on the identified parameters, methods for vibration-based damage detection need to not only be capable of providing parameter estimates for damage identification, but also provide information on the confidence that may be placed on the identification given the partially described, incomplete, and uncertain measurement data provided.

### Issues with Scalability

This approach for fully characterizing the feasible solution space becomes computationally intractable when the dimensionality of the parameter space is significantly increased. Specifically, the boxes of the subpaving tend to accumulate on the boundary due to the amount of bisections required to reach the requested interval precision<sup>38</sup>. Furthermore, the use of the characteristic equation formed through the determinant for the eigenvalue inclusion constraint (Equation 8) does not scale to matrices of higher order. This paper contributes two modifications to the original methodology, described in the following subsections, that permit the approach to be extended to larger multiple degree-of-freedom system models.

**Subpavings vs. Interval Hull** To overcome the issue associated with the computational intractability of subpaving nonlinear problems of large dimensionality, an alternative to subpaving the feasible solution space through bisection and contraction is introduced. Instead of subpaving, a single interval vector solution,  $[\mathbb{X}]$ , called the *interval hull* can be computed, which is a pessimistic enclosure that is guaranteed to contain the exact feasible solution,  $\mathbb{X}$ <sup>38</sup>. The open-source IBEX C++ library<sup>37</sup> provides the ability to contract a box to the interval hull, that is the smallest box enclosing all feasible solutions, with respect to a system of linear inequalities. For problems where the constraint equations are necessarily nonlinear, which is the case for the inverse eigenvalue problem with incomplete mode shape measurement, a means of approximately linearizing the system needs to be provided. In this study, the combined relaxation procedure packaged within the IBEX library that combines a corner-based Taylor relaxation<sup>39</sup> and an affine arithmetic-based relaxation<sup>40</sup> is utilized. The contractor employed is a composition of the forward-backward contraction through the HC4 algorithm<sup>33</sup>, adaptive constructive interval disjunction<sup>41</sup>, and the interval hull contractor, *CtcPolytopeHull*, which calls the linear solver compiled with IBEX (SoPlex<sup>42</sup> in this case) and calculates lower and upper bounds for each variable:

$$\min_{Ax \leq b \wedge x \in [x]} \{x_i\} \quad \text{and} \quad \max_{Ax \leq b \wedge x \in [x]} \{x_i\} \quad (10)$$

The relaxed system is then re-evaluated over the reduced domain and further contracted recursively until a prescribed stopping criterion is reached. The criterion chosen in this study is based on the perimeter of the interval vector that defines the interval hull, which is simply the sum of the widths of each interval solution to the uncertain parameters.

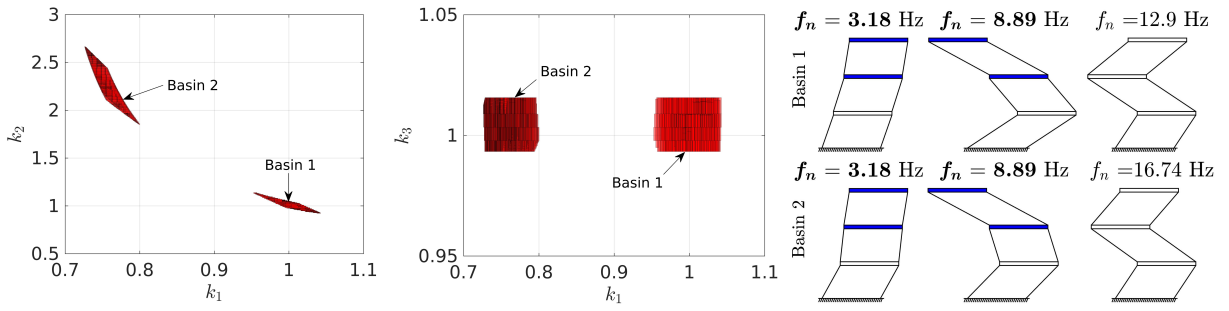


**Figure 3.** Subpavings of the feasible parameter space for the inverse eigenvalue problem subject to partially described, incomplete, and uncertain modal parameters of the three degree-of-freedom system (synthetic measurements of natural frequencies and mode shape coordinates highlighted in bold)

Figure 4 presents the application of the interval hull to enclose the feasible parameter space for the previously described three degree-of-freedom system model with partially described, incompletely measured, and uncertain modal parameter estimates. Comparisons of the interval hull to the subpavings that fully characterize the feasible parameter space reveal that the interval hull provides a complete, although slightly pessimistic, enclosure of the solution basins. In this case, which produced multiple solutions due to the limited data provided, the knowledge of two distinct basins is lost in the interval hull solution. However, the widths of the interval solutions to the uncertain parameters developed through the interval hull still reflect the relative confidence in the estimates of the uncertain parameters, which is sufficient for informing reliable damage detection. For instance, in this case the interval hull contains the expected solution  $k_1 = k_2 = k_3 = 1$  so the solution correctly does not suggest damage in any of the stiffnesses. In terms of computational performance, the interval hull was returned in less than a second of computational time for this problem, which is significantly more efficient than the approach of subpaving.

**Eigenvalue Inclusion Constraint** Since the use of the determinant does not scale to structural systems with larger matrices, an alternative eigenvalue inclusion constraint is developed by leveraging the response surface methodology (RSM) to create a surrogate model for estimating the interval natural frequencies associated with the interval stiffness and mass matrices of the system model. The RSM has been frequently utilized in prior deterministic and probabilistic model updating studies to replace finite element models with approximations that are generally more computationally efficient for estimating the modal properties of parameterized models than eigenvalue decomposition<sup>5,43</sup>. Response surface methodology is a mathematical technique used to establish a relationship between responses,  $y$ , and associated inputs,  $x$ . This relation can be approximated using a polynomial model:

$$y_i = g(x_1, x_2, \dots, x_k)\beta + \epsilon \quad (11)$$

where  $g(\vec{x})$  is a vector consisting of powers and cross-products of unknown input variables,  $\beta$  is a

vector of regression coefficients obtained through the response surface mapping, and  $\epsilon$  is the residual error in the estimate. Typically, either linear or quadratic polynomials are chosen to approximate the relationship between inputs and outputs and interaction terms may be additionally included in these models. For the interested reader, further information about the foundations of response surface methodology can be found in Box and Draper<sup>44</sup>.

In the context of this paper, a response surface is generated from a large set of structural parameters (inputs) and their corresponding responses in the finite element model (output), usually calculated for model updating as the difference between analytical and measured natural frequencies<sup>43</sup>, from which an approximation model is generated by regression. The application of the RSM in this study is used to develop a relationship between the uncertain member stiffnesses,  $\alpha$ , and the corresponding residual error in the natural frequencies of the parameterized model,  $\omega_r - \omega_r^{exp}$ . This equation is represented as,

$$\omega_r - \omega_r^{exp} = g(\alpha_1, \alpha_2, \dots, \alpha_k)\beta \in [-\epsilon, \epsilon] \quad (12)$$

In this study, a set of 1000 unique scalar combinations of member stiffnesses are generated via Latin Hypercube Sampling to ensure an evenly sampled search space and subsequently mapped to a set of outputs in the form of the difference between the natural frequency of the system model and the average measured natural frequency. Multilinear regression is then performed on the set of stiffness scalar combinations and frequency differences to fit a response surface using a quadratic model with interaction terms using the MATLAB Statistics and Machine Learning Toolbox. The regression coefficients and the root-mean-squared-error (RMSE) are extracted to reformulate the eigenvalue inclusion constraint equations from Equation 8 as:

$$\omega_r - \omega_r^{exp} = g(\alpha_1, \alpha_2, \dots, \alpha_k)\beta \in [-\sigma_r, \sigma_r] + [-1.96\text{RMSE}_r, 1.96\text{RMSE}_r] \quad (13)$$

where  $[-1.96\text{RMSE}_r, 1.96\text{RMSE}_r]$  and  $[-\sigma_r, \sigma_r]$  are the 95% confidence interval for the response surface estimate and the standard deviation from the mean

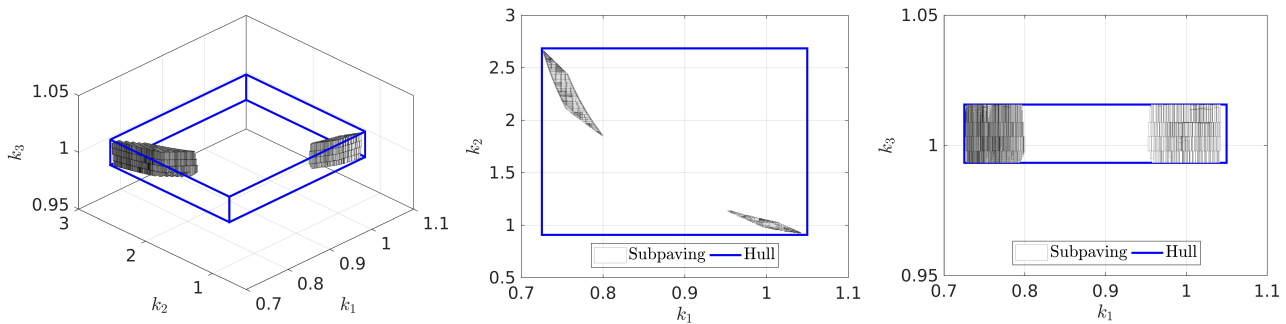


**Figure 4.** Illustration of the use of the interval hull to enclose the feasible parameter space as an alternative to subpavings

for the  $r$ -th natural frequency, respectively. The 95% confidence interval for the response surface estimate is introduced as a relaxation of the constraint equation to account for the potential error introduced by using the response surface as a surrogate for the exact eigenvalue decomposition of the system model.

### Details of Experimental Program for Validation of the Methodology

Recently, hybrid simulation has been explored as an alternative to full-scale vibration testing for structural health monitoring and damage detection<sup>45</sup>. Hybrid testing provides the benefit of limiting the physical testing to only a portion of the structure, while the remainder is strictly numerical and interacts with the experimental member through a substructured form of the dynamic equation of motion. The interaction between the experimental and analytical substructures is illustrated schematically in Figure 5a. This type of testing alleviates the costs associated with full-scale vibration-based damage detection experimentation and, unlike field experimentation where damage is often necessarily simulated through saw cuts or bolt removal, provides a means for faithfully replicating the influence of limit state damage on the dynamic response of the structure. Modeling uncertainties and discretization errors are also alleviated when using hybrid simulation. Consequently, the experiments performed in this paper do not specifically address challenges associated with model and discretization errors in the model updating problem, but rather seek to validate that the methodology is capable of being successfully applied for structural identification and damage detection of well characterized MDOF system models. It should be noted, however, that noise, uncertainties, and nonlinearities are introduced in the hybrid simulation through the experimental measurements obtained from the experimental substructure.

In this paper, hybrid simulation is used to perform vibration testing of a truss model for acquisition of experimental modal analysis data. Between hybrid simulations, realistic damage is progressively introduced in the member of the truss by exceeding a limit state capacity of the experimental substructure. The damage developed in the experimental substructure is the development and progression of fracture cracks at

a bolted connection through net section rupture of the experimental member.

### Details on the Experimental Substructure and Hybrid Simulation

To demonstrate the application of the extended constraint satisfaction-based approach for structural identification using the interval hull, this study employs data from hybrid testing of a simply supported, 45 member 2D Pratt truss with 45 degrees of freedom, shown in Figure 6. All members were modeled as nominally identical A36 steel bars with a gross cross sectional area of 2.42cm<sup>2</sup>. It is noted that the developed methodology is generalized for structural identification of any MDOF system model, including space trusses and frames. A planar truss is used in this paper to aid in interpretation of the results. Forthcoming publications will demonstrate scalability of the methodology to larger and more diverse system models.

The experimental substructure represented a diagonal member of the truss in each experiment and consisted of two 66cm long steel bars with the same gross cross sectional area. The pair of bars was bolted at each end to a 9.5mm thick steel gusset plate using 1.27cm diameter grade 5 bolts and flat washers (Figure 5b). The gusset plates were secured in an MTS 810 universal load testing frame using mechanical wedge grips. Since the mechanical grips displace under changes in load to increase the grip strength, the internal LVDT signal from the load frame could not be utilized for accurate measurement of the specimen elongation. Instead, an RDP Electrosense ACT1000C LVDT was installed between the gusset plates to directly measure the elongation in the experimental substructure. A control loop was established using the LVDT as a feedback signal for strain controlled loading of the experimental substructure that was tuned using the MTS actuator as the control signal. Measurement of the restoring force provided by the experimental member was obtained from the MTS 661.23S-01 load cell on the load frame. Measurements of force and member elongation were acquired with a MTS FlexTest GT controller with Series 493 electronics and were passed to the computer running the hybrid simulation software over a National Instruments X-Series USB data acquisition unit that additionally sent displacement

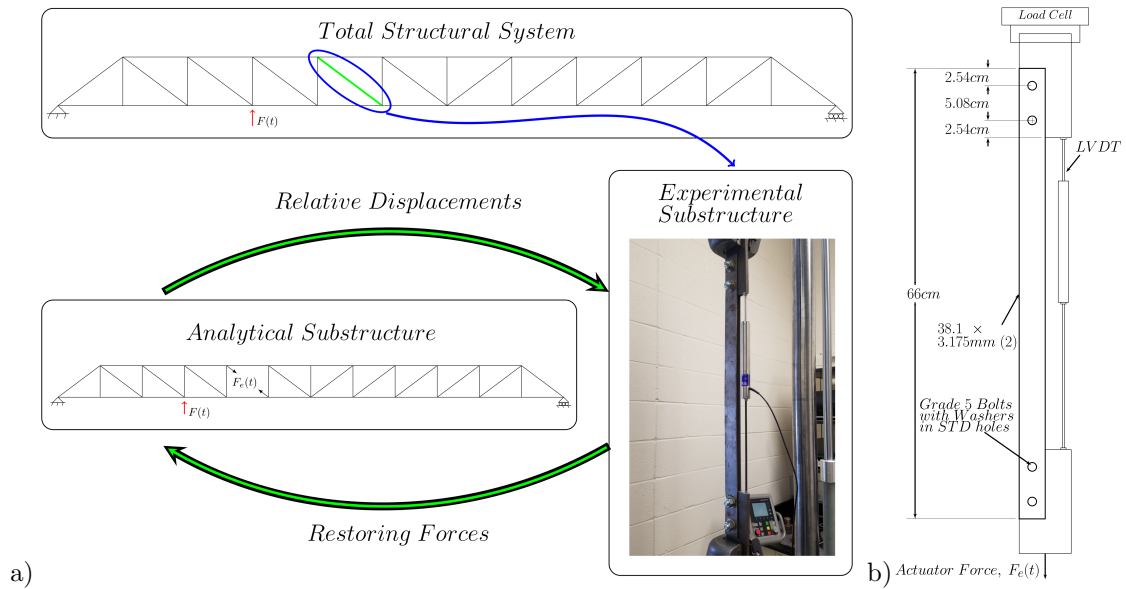


**Figure 5.** a) Schematic of the hybrid simulation applied in the current study, b) details of the experimental substructure and instrumentation

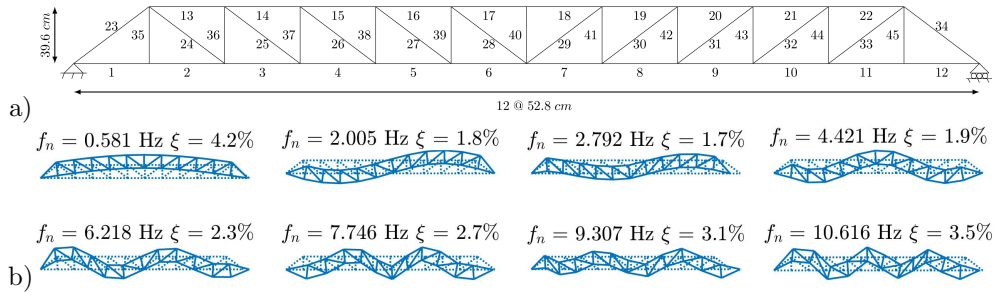


**Figure 6.** a) Forty-five degree-of-freedom Pratt truss used in hybrid testing program for structural identification and damage detection, b) First eight natural frequencies and mode shapes of the truss

commands to the controller using a 16-bit analog output signal. Within the analytical portion of the structure, all members were idealized with pinned connections and linear-elastic material properties, although the hybrid simulation routine accounts for nonlinear geometric effects. The joint masses were scaled and Rayleigh damping was prescribed to generate natural frequencies and damping ratios for the first eight modes of the full structure that are typical for bridges (Figure 6b).

The hybrid simulations were conducted using a MATLAB-based pseudo-dynamic implementation developed in-house and verified in Tedeschi<sup>46</sup>. The hybrid simulation framework incorporates nonlinear geometric effects and implements the incremental-iterative implicit integration scheme developed by Mosqueda and Ahmadizadeh<sup>47</sup>. In the framework, the acceleration is initially assumed to be zero and then iteratively corrected to remove unbalanced forces in the system to converge on a state of dynamic equilibrium. The iterative scheme is used to account for nonlinearities and is performed virtually to avoid unintentional plastic deformations of the experimental substructure. The iterations fit the most

recent force-displacement measurements using second-order polynomials to simulate the virtual response of the experimental substructure while the displacements are iteratively adjusted. Greater details on the hybrid simulation framework may be found in Mosqueda and Ahmadizadeh<sup>47</sup>.

A total of six experimental vibration tests were conducted for the healthy condition and all subsequent damage conditions of the structure through hybrid simulation. Single shaker excitation was applied in the gravity direction at node 4 for three tests and applied in the gravity direction at node 9 for the remaining three tests per condition. A constant force amplitude swept-sine signal was applied over a bandwidth from 0 to 20Hz for a duration of 20 seconds followed by three additional seconds to allow for the free decay response at the end of each test. The amplitude of the applied excitation was scaled such that the stresses in the experimental substructure remained in the linear elastic range. In addition, the experimental member was preloaded prior to each vibration test to simulate the self-weight of the truss and remained in tension throughout the duration of each test. For all vibration tests conducted, a time step of 0.002 seconds was used for the hybrid simulation,

resulting in an effective sampling rate of 500Hz for the measured accelerations.

### *Damage Prescription and Progression*

Following initial vibration testing of the truss with the experimental substructure in the healthy state, the specimen was progressively subjected to static overloading exceeding the limit state capacity to develop cases with increasing extents of damage severity. This overloading was provided through displacement-control loading of the experimental substructure. The force versus elongation response during this overloading is provided in Figure 7a to document the relative reduction in load capacity of the experimental substructure for the first two levels of damage. The first stage of loading developed damage in the form of a single crack on one side of a bolt hole (Figure 7b), while the second stage loading resulted in development and propagation of the crack on both sides of the hole (Figure 7c). For the third damage case, the pair of bars in the experimental substructure consisted of one bar that had completely failed through net section rupture (Figure 7d), while the second bar had not yet developed a crack. Consequently, the reductions in stiffness and strength relative to the healthy condition are expected to be 50% for this case.

An additional benefit of the use of hybrid simulation for experimental vibration-based damage detection research is that the measurement of the force-elongation response of the experimental substructure provides a direct, ground truth measurement of the condition of the damaged member. Figure 8 displays the measured force-elongation response of the experimental substructure acquired during the vibration tests, from which the actual stiffness loss in the experimental member may be estimated. From the change in slope of these responses, it is estimated that the initial damage case resulted in a 7% reduction in the axial stiffness, while the second and third cases produced approximately 12% and 50% reductions, respectively. The hysteresis in the force-elongation response for damage case 3 indicated moderate nonlinearity that is likely a result of slip at the bolted connection for the one bar with complete net section rupture through the cross section.

Since the experimental substructure represented a diagonal member of the truss, it could be used to replace any of the diagonals of the truss in the corresponding analytical model of the hybrid simulation. This ability of hybrid simulation to place the experimental substructure at different locations within the structure was leveraged to validate the methodology over a larger set of cases. For each state of damage, vibration tests were performed where the experimental substructure represented either member 27 or member 31. For each of these tests, the remaining members of the truss were treated as undamaged, but to include cases with damage to multiple members of the truss, two additional sets of vibration tests were performed. In the first, simulated damage was prescribed in member 5 through a 25% reduction in the member stiffness in the analytical model, while real damage remained in the experimental substructure representing member 27.

In the second set, simulated damage was prescribed in both members 8 and 9 through a 25% reduction in the member stiffnesses in the analytical model, while real damage remained in the experimental structure representing member 31. A summary of the damage cases investigated is provided in Table 1.

### *System Identification*

Experimental modal parameter estimates were obtained from the time series data acquired in each test using the combined deterministic stochastic subspace state-space system identification algorithm<sup>48</sup>. Although the hybrid simulation produces acceleration time histories for all of the degrees of freedom in the truss, only those corresponding to a limited sensor array, described in a subsequent section, were used for the system identification. Experimental modal parameter estimates were calculated across a range of model orders and stabilization plots were developed to identify stable estimates according to frequency, damping, and mode shape criteria. If available, five stable poles per mode were selected from each of the six data sets providing a maximum of 30 poles per mode. The standard deviations,  $\sigma$ , of the collected natural frequencies and mode shape components were used to establish interval assignments around the means of the modal property estimates when formulating the constraint equations.

The changes in modal parameter estimates from the healthy state through each damage scenario are summarized in Tables 2 and 3 using the percentage change in natural frequency and modal assurance criterion (MAC). These statistics indicate that the change in global modal properties of the truss with damage is very small, even for the cases where one bar had completely failed through net section rupture. Specifically, for the most severe damage scenario, where the stiffness of the experimental substructure is reduced by half in addition to members 8 and 9 being prescribed 25% stiffness reductions in the analytical model, the largest change in natural frequency across the first eight modes is only 3.4% and the lowest MAC is 0.901. The magnitude of changes in modal parameters observed in this experiment are typical of those that have been observed in field tests of structures<sup>49-51</sup>.

### **Structural Identification**

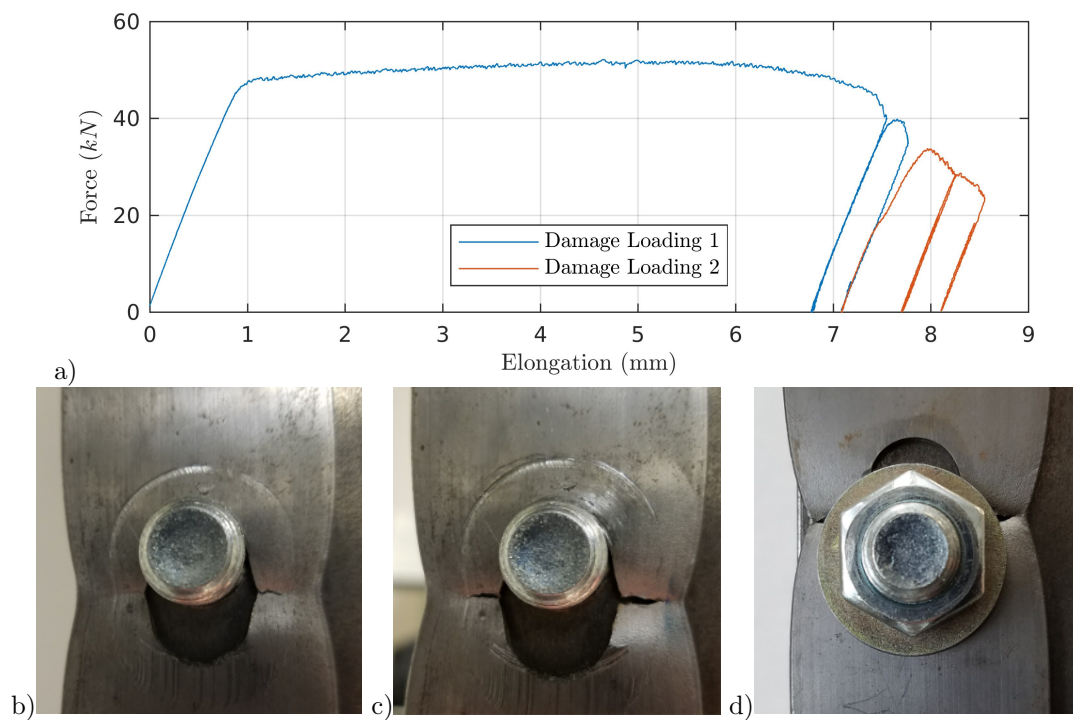
The application of the proposed approach of using constraint satisfaction with interval arithmetic and the interval hull for structural identification will be presented first for the cases where the experimental substructure is in the healthy, undamaged state. Subsequently, application of the methodology for damage detection of the truss across the damage cases in Table 1 will be presented.

### *Parameter Selection and Sensor Layout*

The selection of parameters to include in the model updating routine is of the utmost importance for structural identification as parameters that greatly

**Table 1.** Summary of damage cases investigated (\*represents reduction in analytical portion of hybrid test)

Case	Damage Scenario	Experimental Substructure	Relative Stiffness
1	D0 (no damage)	Member 27	$\alpha_{27} \approx 1.00$
2	D1 (small damage)	Member 27	$\alpha_{27} \approx 0.93$
3	D2 (moderate damage)	Member 27	$\alpha_{27} \approx 0.89$
4	D3 (severe damage)	Member 27	$\alpha_{27} \approx 0.51$
5	D4 (severe + simulated* damage)	Member 27	$\alpha_{27} \approx 0.51, \alpha_5^* = 0.75$
6	D0 (no damage)	Member 31	$\alpha_{31} \approx 1.00$
7	D1 (small damage)	Member 31	$\alpha_{31} \approx 0.94$
8	D2 (moderate damage)	Member 31	$\alpha_{31} \approx 0.89$
9	D3 (severe damage)	Member 31	$\alpha_{31} \approx 0.48$
10	D4 (severe + simulated* damage)	Member 31	$\alpha_{31} \approx 0.48, \alpha_8^* = \alpha_9^* = 0.75$

**Figure 7.** a) Force-elongation curve for the first two damage scenarios of specimen one, b) crack initiation on one side of a bolt hole (specimen one), c) cracking on both sides of bolt hole (specimen one), and d) net section rupture of one bar (specimen two)**Table 2.** Comparison between modal parameter estimates of the healthy structure to each damage case where member 27 was the experimental substructure

Mode	Damage 1		Damage 2		Damage 3		Damage 4	
	$\Delta f(\%)$	MAC						
1	0.003	1.000	0.005	1.000	-0.064	1.000	-1.024	1.000
2	-0.056	1.000	-0.115	1.000	-0.793	1.000	-1.865	0.999
3	0.000	1.000	-0.002	1.000	-0.029	1.000	-0.150	1.000
4	-0.176	1.000	-0.316	1.000	-2.307	0.996	-2.412	0.996
5	-0.006	1.000	-0.015	1.000	-0.040	1.000	-1.102	0.999
6	-0.138	1.000	-0.291	1.000	-1.829	0.986	-2.403	0.983
7	-0.013	1.000	-0.026	1.000	-0.092	0.998	-0.145	0.996
8	-0.344	0.999	-0.629	0.998	-4.122	0.929	-4.135	0.932

affect the modal properties should be included, while parameters that have negligible effect should be excluded for the sake of computational efficiency. The selection of parameters is also dependent on

the sensor layout, as the uniqueness of the inverse problem depends on the availability of the partially described and incompletely measured modal parameter estimates. Existing methods for parameter selection

**Table 3.** Comparison between modal parameter estimates of the healthy structure to each damage case where member 31 was the experimental substructure

Mode	Damage 1		Damage 2		Damage 3		Damage 4	
	$\Delta f(\%)$	MAC						
1	-0.004	1.000	-0.025	1.000	-0.145	1.000	-1.732	1.000
2	-0.005	1.000	-0.007	1.000	-0.044	1.000	-1.272	0.998
3	-0.014	1.000	-0.023	1.000	-0.274	0.999	-1.611	0.998
4	-0.182	1.000	-0.331	1.000	-2.541	0.993	-2.844	0.991
5	-0.133	1.000	-0.274	1.000	-1.399	0.992	-1.601	0.989
6	-0.050	1.000	-0.089	1.000	-0.305	0.998	-2.220	0.990
7	-0.076	1.000	-0.122	1.000	-0.564	0.993	-1.187	0.978
8	-0.089	1.000	-0.226	0.998	-1.874	0.888	-3.405	0.901

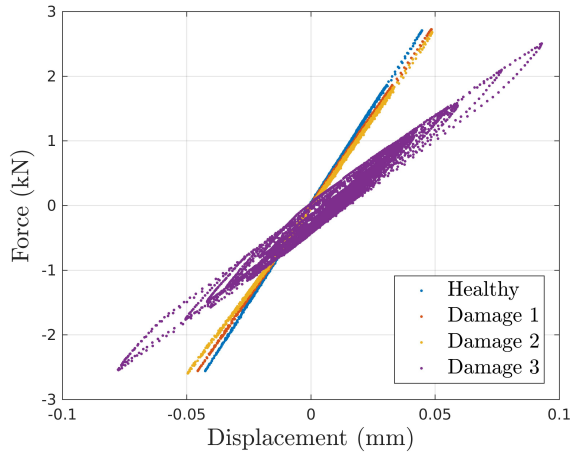


**Figure 8.** Force-elongation histories for healthy and damage cases for the experimental substructure

have often relied on sensitivity analyses and/or substructuring to significantly narrow down the set of uncertain parameters to a mere handful of structural properties<sup>52</sup>. In the current study, a sensitivity analysis revealed that the vertical members of the truss had little impact on the first eight natural frequencies and mode shapes. Consequently, the stiffnesses of these members were excluded from the structural identification, while the remaining horizontal and diagonal members were considered as potential candidates for parameter identification. The final set of uncertain parameters included in the subsequent structural identifications was determined through a parameter identifiability study informed by the sensor layout.

As previously stated, it is impractical/impossible to physically measure all degrees of freedom of a model. In this study, a total of 23 sensor axes were used over the 45 unrestrained degrees of freedom of the truss (Figure 9a) to provide incomplete measurement of the mode shapes. Parameter identifiability was assessed using purely analytical modal parameters for the first eight modes, although small uncertainty of  $\pm 0.0001$  was introduced on the normalized “measured” mode shape components. The extended methodology for structural identification using nonlinear constraint satisfaction with interval arithmetic was applied using the analytical data with an initial search space for each stiffness parameter covering the range of 0.5 to 1.5. Figure 9b presents the

interval hull solution for the horizontal and diagonal members obtained from the structural identification, which indicates that the available partially described and incompletely measured modal parameter estimates acquired from the sensor configuration are capable of identifying the stiffness of all diagonal members and all but six of the horizontal members. The unidentifiable nature of these parameters, as indicated by the inability of the constraint solver to shrink the domains of these variables, can logically be attributed to the sparsity of the sensor layout around these members. As a result of the parameter identifiability, all verticals and these six horizontal members were excluded from all subsequent identification, and the scalar stiffness multiplier for each of these members,  $\alpha$ , was set to one leaving a total of 28 remaining member scalar stiffness assignments as unknown parameters.

### Identification of the Undamaged Case Using the Interval Hull

The extended methodology of structural identification through nonlinear constraint satisfaction with interval arithmetic was first applied to the experimental modal parameter estimates acquired from the two cases obtained from the healthy structure to validate the approach. For both cases, the eigeninformation was limited to the first eight modes and the 28 aforementioned stiffness scalars were treated as unknowns. However, given the incomplete mode shape measurement, an additional 176 unmeasured components of the mode shapes arise as additional unknowns, creating a 204-dimensional search space. To incorporate measurement uncertainty into the problem, the measured eigenvector components were prescribed as intervals,  $[\phi_{i,r}^{avg} - \sigma_{\phi_{i,r}}, \phi_{i,r}^{avg} + \sigma_{\phi_{i,r}}]$  where  $\phi_{i,r}^{avg}$  and  $\sigma_{\phi_{i,r}}$  are the average and standard deviation of the normalized experimental estimate of the  $i$ -th degree of freedom of the  $r$ -th mode shape, respectively. However, consistent with Equation 6, the component with the maximum amplitude for each mode was prescribed the degenerate interval  $[1,1]$  to anchor the eigenvector, since the amplitude of an eigenvector is not unique. In this implementation, the eigenvalues were prescribed exactly as the confidence intervals for the response surface models for the eigenvalue inclusion constraint exceeded the standard deviation of the individual natural frequency estimates by an order of magnitude.

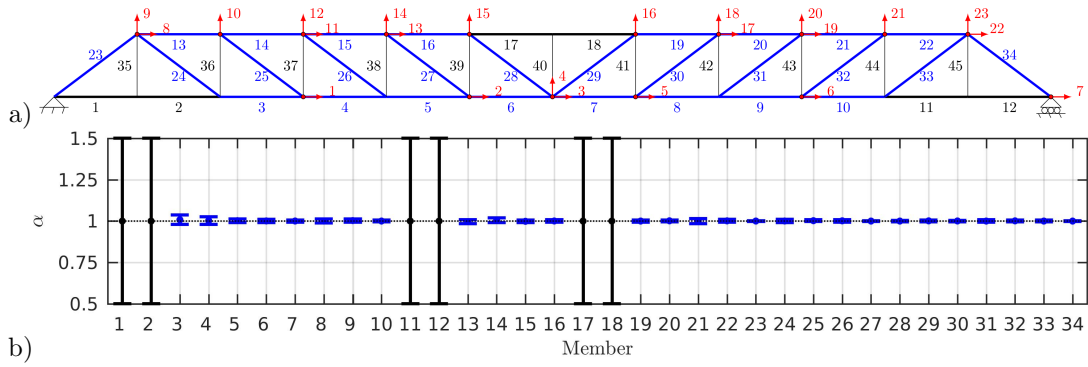


**Figure 9.** a) Sensor layout chosen to identify all of the diagonal and horizontal members of the truss b) Determination of identifiable diagonal and horizontal members based on the interval hull

The search space for the unknown stiffness parameters was bounded to  $\alpha_k \in [0.25, 1.5]$ , where a value of 1 represents no change from the baseline assumption, while the unmeasured components of the mode shape were bounded to  $\phi_{j,r} \in [-10, 10]$ .

The constraint equations generated by Equations 3 and 13 using the first 8 natural frequencies and corresponding incomplete mode shapes of the healthy structure were passed to the developed interval hull solver and the domain of the unknown parameters was contracted until the perimeter of the search space, that is the sum of the widths of each interval, changed less than 0.0001 between two consecutive interval hull contractions. Figure 10 displays the calculated interval hull obtained for the healthy case where member 27 was represented by the experimental substructure. Although the set of 204 unknown parameters was significantly large, especially with respect to traditional FE model updating techniques, the proposed approach was able to successfully contract the interval hull in approximately 20 minutes of computational time to identify the uncertain stiffness parameters. As illustrated in the figure, each interval solution for the stiffness parameters correctly contains the nominal stiffness of the healthy members associated with  $\alpha=1$ . The width of each interval in the hull reflects the confidence in each parameter estimate and is guaranteed to be a complete enclosure, or superset, of the feasible parameter range under the prescribed constraints and measurement uncertainty. The propagation of measurement uncertainties to the parameter domain is reflected in uncertainties in the identified parameters on the order of a few percent. In addition to the uncertain stiffness parameters, the 176 additional unknown eigenvector components were also returned with similarly narrow intervals.

To verify the solution, the upper and lower bounds of the identified stiffness parameters were used to construct an interval stiffness matrix for the structure and the approach in Modares et al.<sup>53</sup> was utilized to determine the interval natural frequencies of the identified model. Table 4 presents these interval natural frequencies, which confirms that the identified model constructed by the interval hull correctly encompasses the eight

prescribed natural frequencies associated with the healthy model. Most of the interval natural frequencies are centered about the experimental estimates and the width of all of the intervals are within 1% of the experimental values. Similar results were obtained when the undamaged experimental substructure was used to represent member 31 of the truss (Figure 11).

### Identification of the Damaged Cases Using the Interval Hull

To demonstrate the capabilities of the proposed method for damage detection applications, the same methodology applied in the identification of the undamaged cases was applied to the data sets acquired for the remaining eight damaged cases in Table 1. The constraint equations generated by Equations 3 and 13 were generated with the experimental modal parameter estimates for each case and passed to the developed interval hull solver. As in the prior analysis, the domain of the resulting 207 unknown parameters was contracted until the perimeter of the search space changed less than 0.0001 between two consecutive interval hull contractions. Figure 12 displays the solutions for the interval hulls for the damaged cases where the experimental substructure represented member 27 of the truss. In all cases of damage, the proposed method clearly and correctly identifies member 27 as the damaged element. In addition, Table 5 presents the interval solutions for the scalar stiffness parameter of member 27, which shows that the identified extent of damage agrees well with the expected stiffness loss calculated by the change in slope of the force-elongation responses of the experimental substructure. It should also be noted that it can be stated with certainty that there is a loss of stiffness in the experimental substructure since  $\alpha = 1$  is not an element of the identified intervals. Additionally, Figure 12 illustrates that, even when the uncertainty in the identified stiffness parameters for the undamaged members increases at the damage 3 severity due to the significant nonlinearity in the damaged experimental substructure (Figure 12c), it cannot be stated with certainty that the stiffness of the undamaged elements has changed since  $\alpha = 1$  is a member of the identified

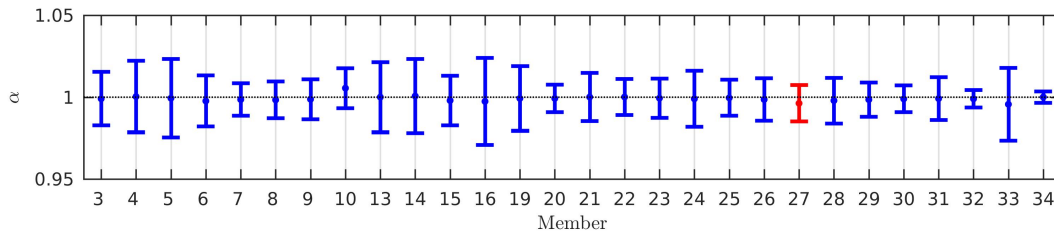


**Figure 10.** Interval hull solution for the stiffness scalars with member 27 as the experimental substructure and tested in the healthy condition

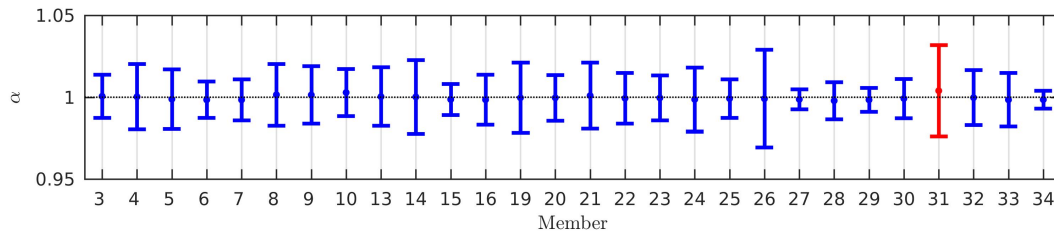


**Figure 11.** Interval hull solutions for the stiffness scalars with member 31 as the experimental substructure and in the healthy condition

intervals for those parameters. Furthermore, the means of the identified intervals for the stiffness of the undamaged parameters are nearly centered around one. For case 5, where the stiffness of element 5 was decreased by 25% in the analytical portion of the structure, the proposed approach correctly identified the severity of damage for both elements 5 and 27 of the truss (Figure 12d).

Results for the cases where the experimental substructure represented member 31 of the truss are presented in Figure 13 and Table 5. As in the prior cases, the interval hull solutions in all four damage cases clearly and correctly identify the damaged element. However, for case 9, where only member 31 is damaged, it cannot be stated with certainty that no other members are damaged given the specified measurement uncertainty. As illustrated in Figure 13c, the identified interval solutions for the stiffness of members 8 and 9 do not contain  $\alpha = 1$ , which lies just outside of the intervals. For case 10, which was performed using new measurement data where elements 8 and 9 were artificially subjected to 25% losses in stiffness in addition to the experimentally damaged member 31, the proposed approach clearly and correctly identified the location and severity of damage, while providing no misidentification of undamaged elements as damaged under the specified measurement uncertainty (Figure 13d).

The false positive identification of minor damage (less than 5% stiffness change) in the two members in case 9 is attributed to the significant nonlinearity in the response of the experimental substructure at this extent of damage severity coupled with the sparsity of sensors in proximity of the damaged member. Both incorrectly classified members are connected to the damaged member at the same node and no sensor axes are located at this node. As previously

detailed, the measurement uncertainty for the structural identification was prescribed using the standard deviations of the normalized experimental eigenvector components. If the interval bound for the experimental modal parameter estimates is slightly increased by specifying the uncertainty on the experimental modal parameter estimates as  $\pm 1.125\sigma$ , the only identified interval solution for the stiffness parameters that does not contain  $\alpha = 1$  is that of the damaged member (Figure 14). Comparisons of the identified interval solutions for the stiffness parameters produced with different uncertainty bounds also highlight the ability of the methodology to quantify the parameter sensitivities to the measurement uncertainty, as the expansion in width of the interval vector solution varies across individual stiffness parameters. Parameter sensitivities depend on the richness of the experimental modal parameter estimates (number and location of sensor axes and number of identified modes), the quality of the experimental modal parameter estimates, and the extent to which the physical response of the structure adheres to or violates the underlying assumptions in the system model. Notably, the largest increases in interval widths for this example are observed for top and bottom chord members in proximity of the experimental substructure exhibiting the nonlinear damage. Ultimately, specific confidence intervals could be associated with the measurement uncertainties specified in the constraint equations employed in the developed structural identification methodology if knowledge of the distributions of the experimental modal parameters is available. However, these distributions may be non-normal<sup>54</sup> and therefore not readily estimated from the variances. Furthermore, the determination of confidence intervals for non-normal distributions of modal parameters of large civil

**Table 4.** Comparison between experimental natural frequencies and interval natural frequencies of the identified model for case 1

Mode	$f_{exp}$	$[f, \bar{f}]$	$[\Delta f(\%), \Delta \bar{f}(\%)]$
1	0.581	[0.577, 0.584]	[-0.803, 0.531]
2	2.005	[1.991, 2.017]	[-0.685, 0.622]
3	2.792	[2.777, 2.805]	[-0.519, 0.485]
4	4.421	[4.393, 4.448]	[-0.634, 0.599]
5	6.218	[6.180, 6.255]	[-0.614, 0.595]
6	7.746	[7.716, 7.777]	[-0.391, 0.399]
7	9.307	[9.262, 9.357]	[-0.482, 0.529]
8	10.616	[10.553, 10.687]	[-0.587, 0.671]

structures presents several challenges<sup>55</sup> that currently have not been fully addressed in the literature.

## Conclusion

Extensions of a newly developed method for structural identification using nonlinear constraint satisfaction with interval arithmetic have been presented to permit the approach to be applied to larger MDOF system models. The basis of the extended formulation relies on foregoing computation of a complete set of feasible solutions and instead contracts the search domain to the interval hull, which encompasses the complete set of feasible solutions with a single interval vector solution. The use of interval analysis in the methodology has been leveraged to account for measurement and model uncertainties. In addition, a response surface model was introduced to allow for enforcement of an eigenvalue inclusion constraint equation while still enabling interval contraction over the constraint equations.

Hybrid simulation was utilized for acquisition of vibration data from both healthy and damaged states of a planar truss structure subjected to realistic structural damage. In this paper, a two-bar specimen with bolted connections representing a single member of the truss served as the experimental substructure. Multiple sets of vibration data were acquired for each damage state from which the standard deviations about the means of the modal parameter estimates were used to establish interval assignments in the constraint equations. Application of the methodology to data from the undamaged structure demonstrated the ability of the constraint satisfaction approach to identify the subset of identifiable parameters in the model subject to the measurement data and validated that the response surface methodology introduced into the eigenvalue inclusion constraint correctly constrained the interval hull solutions to enclose the measured natural frequencies. In addition to correctly identifying the uncertain stiffness parameters in the undamaged case, the proposed methodology provided accurate damage identification for all cases of severity without misidentifying undamaged members as damaged, except in a single case where the two members directly connected to the severely damaged member were identified as having minor changes in stiffness. The ability of the methodology to quantify the sensitivity

of uncertain parameters in the model to measurement uncertainties was also demonstrated through expansion of the interval bounds used to specify the measurement uncertainty. With a nominal increase in the specified measurement uncertainty, the two false positives were rectified with no appreciable effect on the identification of the stiffness of the damaged member.

## Acknowledgements

This material is based upon work supported by the National Science Foundation under Grant No. 1331825. Any opinions, findings, conclusions, or recommendations expressed in the material are those of the authors and do not necessarily reflect the views of the sponsor.

## References

1. Simoen E, Roeck GD and Lombaert G. Dealing with uncertainty in model updating for damage assessment: A review. *Mechanical Systems and Signal Processing* 2015; 56-57: 123–49.
2. Chu M and Golub G. *Inverse Eigenvalue Problems: Theory, Algorithms, and Applications*. 2005.
3. Beck JL and Katafygiotis LS. Updating models and their uncertainties. I: Bayesian statistical framework. *Journal of Engineering Mechanics* 1998; 124(4): 455–461.
4. Beck JL and Au SK. Bayesian updating of structural models and reliability using Markov Chain Monte Carlo simulation. *Journal of Engineering Mechanics* 2002; 128: 380–391.
5. Marwala T. *Finite-element-model updating using computational intelligence techniques*. Springer, 2010.
6. Zhang J, Wan C and Sato T. Advanced Markov Chain Monte Carlo approach for finite element calibration under uncertainty. *Computer-Aided Civil and Infrastructure Engineering* 2013; 28: 522–530.
7. Behmanesh I and Moaveni B. Probabilistic identification of simulated damage on the Dowling Hall footbridge through Bayesian finite element model updating. *Structural Control and Health Monitoring* 2015; 22(3): 463–483. STC-13-0111.R2.
8. Sun H and Büyüköztürk O. Probabilistic updating of building models using incomplete modal data. *Mechanical Systems and Signal Processing* 2016; 75(Supplement C): 27 – 40.
9. Goller B, Beck JL and Schuëller GI. Evidence-based identification of weighting factors in Bayesian model updating using modal data. *Journal of Engineering Mechanics* 2012; 138(5): 430–440.
10. Sohn H and Law KH. A Bayesian probabilistic approach for structure damage detection. *Earthquake Engineering and Structural Dynamics* 1997; 26(12): 1259–1281.
11. Vanik MW, Beck JL and Au SK. Bayesian probabilistic approach to structural health monitoring. *Journal of Engineering Mechanics* 2000; 126(7): 738–745.
12. Yuen KV, Beck JL and Au SK. Structural damage detection and assessment by adaptive Markov Chain Monte Carlo simulation. *Structural Control and Health Monitoring* 2004; 11(4): 327–347.

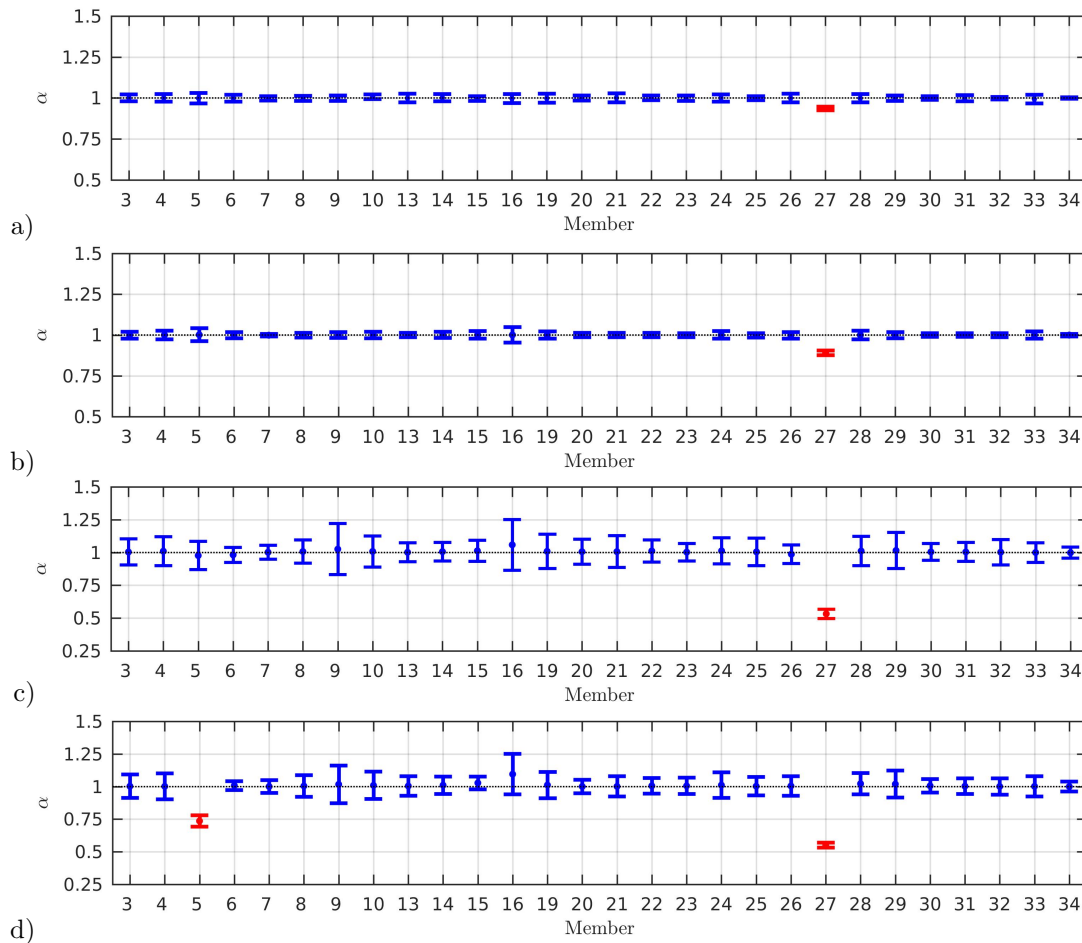


**Figure 12.** Interval hull solutions for the stiffness scalars with the experimental substructure representing member 27 a) damage case D1, b) damage case D2, c) damage case D3, and d) damage case D4, where member 5 was subjected to a 25% stiffness reduction in the analytical model

**Table 5.** Comparison between expected stiffness parameter estimates to those identified by the interval hull for both experimental substructures and all damage cases (\* represents the cases with significant nonlinearity in the force-elongation response)

Member 27	Expected $\alpha$	Identified $\alpha$	Member 31	Expected $\alpha$	Identified $\alpha$
Healthy	1.000	[0.985, 1.007]	Healthy	1.000	[0.976, 1.032]
Damage 1	0.935	[0.925, 0.948]	Damage 1	0.937	[0.921, 0.966]
Damage 2	0.887	[0.877, 0.905]	Damage 2	0.886	[0.848, 0.937]
Damage 3	0.509*	[0.496, 0.568]	Damage 3	0.483*	[0.556, 0.587]
Damage 4	0.509*	[0.530, 0.570]	Damage 4	0.483*	[0.481, 0.600]

13. Yuen KV, Beck JL and Katafygiotis LS. Unified probabilistic approach for model updating and damage detection. *Journal of Applied Mechanics* 2005; 73.
14. Ching J, Muto M and Beck JL. Structural model updating and health monitoring with incomplete modal data using Gibbs sampler. *Computer-Aided Civil and Infrastructure Engineering* 2006; 21(4): 242–257.
15. Huang Q, Gardoni P and Hurlbauss S. A probabilistic damage detection approach using vibration-based nondestructive testing. *Structural Safety* 2012; 38: 11 – 21.
16. Mustafa S and Matsumoto Y. Bayesian model updating and its limitations for detecting local damage of an existing truss bridge. *Journal of Bridge Engineering* 2017; 22(7): 04017019.
17. Biswal S and Ramaswamy A. Damage identification in concrete structures with uncertain but bounded measurements. *Structural Health Monitoring* 2017; 16(6): 649–662.
18. Behmanesh I, Moaveni B and Papadimitriou C. Probabilistic damage identification of a designed 9-story building using modal data in the presence of modeling errors. *Engineering Structures* 2017; 131: 542 – 552.
19. Köyliüoğlu HU, Çakmak AŞ and Nielsen SRK. Interval algebra to deal with pattern loading and structural uncertainties. *Journal of Engineering Mechanics* 1995; 121: 1149–1157.

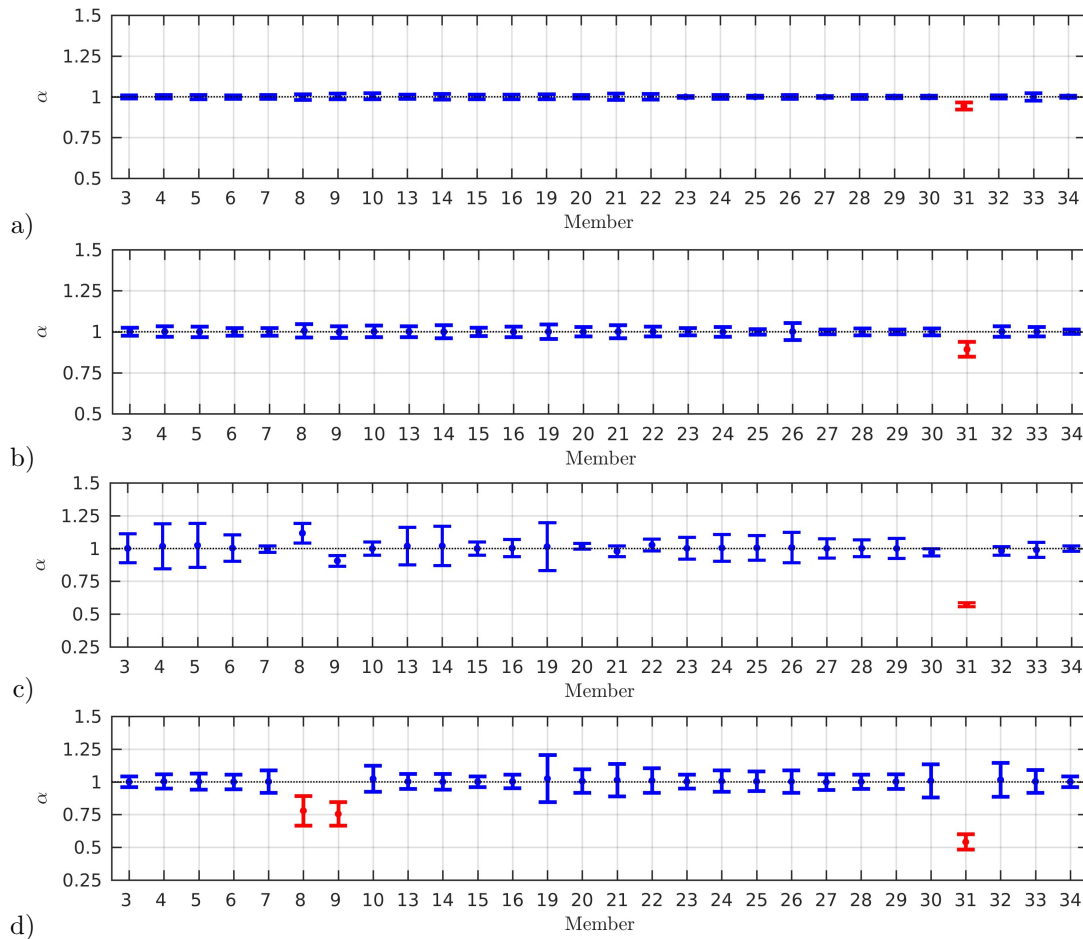


**Figure 13.** Interval hull solutions for the stiffness scalars with the experimental substructure representing member 31 a) damage case D1, b) damage case D2, c) damage case D3, and d) damage case D4, where members 8 and 9 were subjected to 25% stiffness reductions in the analytical model

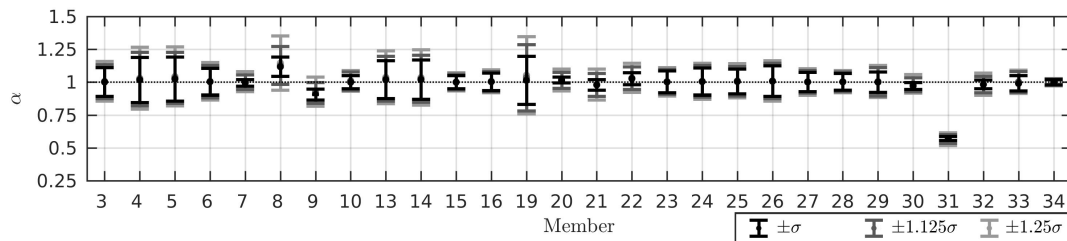


**Figure 14.** Interval hull solutions for the stiffness scalars with the experimental substructure representing member 31 for damage case D3 with increasing interval bounds on the uncertainty of the experimental modal parameter estimates

20. Gabriele S, Valente C and Brancaleoni F. An interval uncertainty based method for damage identification. In *Damage Assessment of Structures VII, Key Engineering Materials*, volume 347. Trans Tech Publications, pp. 551–556.
21. Wang X, Yang C, Wang L et al. Membership-set identification method for structural damage based on measured natural frequencies and static displacements. *Structural Health Monitoring* 2013; 12: 23–34.
22. Wang X, Yang C and Qiu ZP. Non-probabilistic information fusion technique for structural damage identification based on measured dynamic data with uncertainty. *Acta Mechanica Sinica* 2013; 29: 202–210.
23. Khodaparast HH, Mottershead JE and Badcock KJ. Interval model updating with irreducible uncertainty using the Kriging predictor. *Mechanical Systems and Signal Processing* 2011; 25: 1204–1226.
24. Fang SE, Zhang QH and Ren WX. An interval model updating strategy using interval response surface models. *Mechanical Systems and Signal Processing* 2015; 60-61: 909–927.
25. Gabriele S and Valente C. An interval-based technique for FE model updating. *International Journal of Reliability and Safety* 2009; 3: 79–103.
26. Gabriele S. The interval intersection method for FE model updating. *Journal of Physics: Conference Series* 2011; 305.

27. Kernicky T, Whelan M, Rauf U et al. Structural identification using a nonlinear constraint satisfaction processor with interval arithmetic and contractor programming. *Computers and Structures* 2017; 188: 1–16.
28. Rossi F, van Beek P and Walsh T. *Handbook of Constraint Programming (Foundations of Artificial Intelligence)*. Elsevier Science, 2006.
29. Hyvnen E. Constraint reasoning based on interval arithmetic: the tolerance propagation approach. *Artificial Intelligence* 1992; 58: 71–112.
30. Dechter R. *Constraint Processing*. 1 ed. Morgan Kaufmann, 2003.
31. Hentenryck PV. *The OPL Optimization Programming Language*. MIT PRESS, 1999.
32. Alefeld G and Claudio D. The basic properties of interval arithmetic, its software realizations and some applications. *Computers & Structures* 1998; 67(1): 3–8.
33. Benhamou F, Goualard F, Granvilliers L et al. Revising hull and box consistency. In *Logic Programming: Proceedings of the 1999 International Conference on Logic Programming*. MIT press, p. 230.
34. Chabert G and Jaulin L. Contractor programming. *Artificial Intelligence* 2009; 173(11): 1079–1100.
35. Benhamou F and Granvilliers L. Automatic generation of numerical redundancies for non-linear constraint solving. *Reliable Computing* 1997; 3(3): 335–344.
36. MATLAB. *version 8.6.0 (R2015b)*. Natick, Massachusetts: The MathWorks Inc., 2015.
37. Chabert G. IBEX C++ library for constraint processing over real numbers, 1999. URL <http://www.ibex-lib.org>.
38. Jaulin L, Kieffer M, Didrit O et al. *Applied Interval Analysis*. Springer, 2001.
39. Araya I, Trombettoni G and Neveu B. *A Contractor Based on Convex Interval Taylor*. Berlin, Heidelberg: Springer Berlin Heidelberg, 2012. pp. 1–16.
40. Ninin J, Messine F and Hansen P. A reliable affine relaxation method for global optimization. *4OR* 2015; 13(3): 247–277.
41. Neveu B, Trombettoni G and Araya I. Adaptive constructive interval disjunction: algorithms and experiments. *Constraints* 2015; 20: 452–467.
42. SoPlex. Sequential object-oriented simplex, 2017. URL <http://soplex.zib.de/>.
43. Ren WX and Chen HB. Finite element model updating in structural dynamics by using the response surface method. *Engineering Structures* 2010; 32(8): 2455 – 2465.
44. Box G and Draper N. *Empirical Model-Building and Response Surfaces*. Wiley, 1987.
45. Kernicky TP, Tedeschi M and Whelan MJ. *Leveraging Hybrid Simulation for Vibration-Based Damage Detection Studies*. Springer International Publishing, 2016. pp. 333–341.
46. Tedeschi M. *Development, verification, and validation of a hybrid testing framework for latticed structures with nonlinear geometric effects*. Master’s Thesis, University of North Carolina at Charlotte, 2015.
47. Mosqueda G and Ahmadizadeh M. Iterative implicit integration procedure for hybrid simulation of large nonlinear structures. *Earthquake Engineering and Structural Dynamics* 2011; 40(9): 945–960.
48. VanOverschee P and DeMoor B. *Subspace Identification for Linear Systems, Theory–implementation–applications*. Dordrecht: Kluwer Academic Publishers, 1996.
49. Farrar C, Baker W, Bell T et al. Dynamic characterization and damage detection in the I-40 bridge over the rio grande. Technical report, Los Alamos National Laboratory.
50. Alampalli S, Fu G and Dillon EW. Signal versus noise in damage detection by experimental modal analysis. *Journal of Structural Engineering* 1997; 123(2): 237–245.
51. Brincker R, Andersen P and Cantieni R. Identification and level I damage detection of the Z24 highway bridge. *Experimental Techniques* ; 25(6): 51–57.
52. Moaveni B, Stavridis A, Lombaert G et al. Finite-element model updating for assessment of progressive damage in a 3-story infilled RC frame. *Journal of Structural Engineering* 2013; 139: 1664–1674.
53. Modares M, Mullen RL and Muhanna RL. Natural frequencies of a structure with bounded uncertainty. *Journal of Engineering Mechanics* 2006; 132(12): 1363–1371.
54. Tondreau G and Deraemaeker A. Numerical and experimental analysis of uncertainty on modal parameters estimated with the stochastic subspace method. *Journal of Sound and Vibration* 2014; 333(18): 4376–4401.
55. Carden E and Mita A. Challenges in developing confidence intervals on modal parameters estimated for large civil infrastructure with stochastic subspace identification. *Structural Control and Health Monitoring* 2011; 18(1): 53–78.